



# Fusion welding thermal simulation in corrugated steel for one-way slabs

J. Ferreiro-Cabello<sup>1\*</sup>, E. Fraile-Garcia<sup>1</sup>, E. Fernández González<sup>1</sup>, C. Gonzalez-Gonzalez, E. Jimenez Macias<sup>1</sup>

<sup>1</sup>University of La Rioja, Luis de Ulloa 4, Logroño (La Rioja), 26004, Spain

\*Corresponding author. Email address: [javier.ferreiro@unirioja.es](mailto:javier.ferreiro@unirioja.es)

## Abstract

The objective of this work is to carry out a study on fusion welding by modifying different variables: pressures, intensity and time. This process will be used for the elaboration of rebar in reinforced concrete structures such as unidirectional slabs. Currently, the corrugated steel bars used in the construction sector are usually welded using MIG (Metal Inert Gas) welding. This welding emits gases that are harmful to the environment and to welders. For this reason, an attempt is made to find a better alternative for rebar welding. After studying the current welding methods, it was decided to test the effectiveness of electric resistance welding because it is a cleaner weld, the main reason being that it does not use material or filler gases. The methodology followed to verify the effectiveness of the new alternative consists of the elaboration of several test pieces combining corrugated steel bars of different diameters joined through spot welding, carried out by electric resistance welding. The welding process is recorded with a thermographic camera, to obtain the maximum temperature during said process, of all the combinations studied. To determine if welding with the new alternative is thermally feasible. The results allow to determine that the welding is feasible with the new alternative. All the experiments are validated by a finite-elements simulation, and, once the model is validated, more range of values are obtained using simulation without price increase.

**Keywords:** Modelling structures, Reinforced concrete, Structural steel, thermal simulation, one-way slabs.

## 1. Introduction

In the construction sector there are many subsectors, one of them are the companies specialized in the supply of materials related to rebar such as beams, walls, grills, bands, foundation reinforcement... Currently, the environment and safety are Two very important factors to consider. This translates into the importance of the rational use of resources, reducing



emissions of harmful gases for the planet and for workers. Therefore, different concerns are combined: on the one hand, trying to offer construction products that meet the current demands set out in the Technical Building Code and, on the other, the awareness of betting on sustainable and healthy construction.

In this work, simulation is used to validate the experimental results obtained and the experiments developed. A figure of the real system is not included since they do not contribute to a better understanding of the system and its behavior; however the information from tables and graphs provides the reader with a concrete idea of the system. The idea of using real stimulation to feed the simulation model is close to the idea of digital twins, although in this paper such paradigm is not formally used.

## 2. State of the art

Numerous studies deal with sustainability in construction, in reinforced concrete structures [1], in unidirectional slabs [2], in elements such as precast slabs incorporating cardboard [3], in residential building pillars [4], more specifically there are also environmental studies on the repercussion of steel in reinforced concrete columns [5]. The combination of these two concerns led to the search for innovative solutions that provide buildings with energy efficiency and improve comfort parameters. All this with a basic principle that is also the social repercussion of the proposed solutions. This social aspect is not negligible as its impact on the local economy can be extraordinarily important. The objective is to focus on the search for alternatives that, without neglecting the means available at the local level, allow us to face these new challenges currently posed. Given the current situation in the construction sector, innovation and differentiation can be a critical factor for the companies, which must take advantage of the current situation to improve and rethink their production processes. These factors are currently led by eco-efficiency, its impact on energy consumption and therefore on the economy is immediate, but additional factors such as acoustic comfort, sustainability and occupational health and safety should not be neglected.

The idea of using both model and system to develop a kind of digital system [6], has been used in welding combined with artificial intelligence, as for instance in [7-9], and is a very well known way to characterization of materials and welding processes [10-12].

Therefore, the project seeks a technically viable alternative that is capable of replacing the welding machines currently used in rebar assembly with a less polluting one with a lower production cost. Focusing mainly on determining if with this welding process, the physical and chemical properties of the steel are maintained.

## 3. Materials and Methods

The research focuses on the study of fusion welding of corrugated steel bars as reinforcement for concrete structures. According to current regulations UNE-EN 10080, the possible nominal diameters are 6, 8, 10, 12, 14, 16, 20, 25, 32 and 40 mm. Being the most used in the steel industry the diameters from 8 to 20 mm. The types of steel used are weldable steels (B 400 S and B 500 S) and weldable steels with special ductility characteristics (B 400 SD and B 500 SD).

This work it tries to determine, using simulation models and experiments, if the physical and chemical properties of the steel are affected during the fusion welding process. This will be determined based on the maximum temperature reached in the weld. The steel used in this study is B-500-SD, the characteristics of the material comply with what is specified in the UNE 36065:2011 standard and whose values are shown in tables 1 and 2.

Table 1. Chemical Composition Steel B 500 SD

C (%)	S (%)	P (%)	N (%)	Ceq (%)
0,220	0,050	0,050	0,012	0,500

Table 2. Mechanical Characteristics Steel B 500 SD

Re (MPa)	Rm (MPa)	Rm/Re	A5 (%)	Dob/Desd	Agt (%)
>=500	>=575	1,15-1,35	>=16	0,500	>=10

It is a steel with a low percentage of carbon (0.22%), as can be seen in the Iron-Carbon diagram (figure 1), it is a Hypoeutectoid steel:

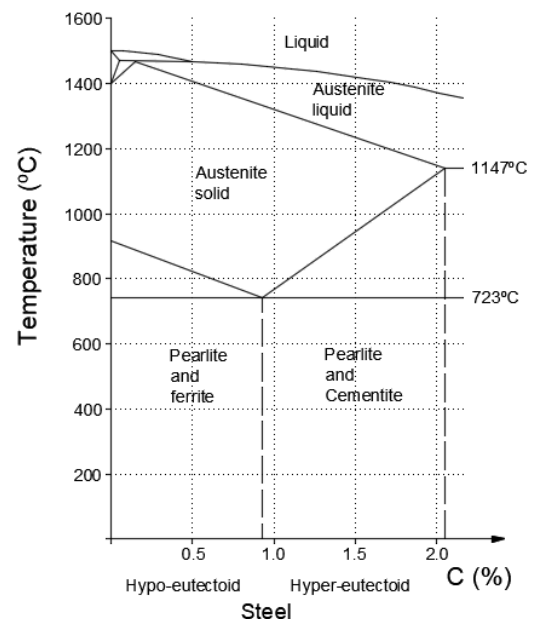


Figure 1. Iron Carbon Diagram

The welds are made with the "MPH Digital Pneumatic" welding equipment. This equipment, regulated by means of an electronic control system by thyristors, allows to modify: the welding point time, the power used and the pressure of the electrodes. The digital controller allows parameter adjustments to be made in a simplified way, with the possibility of carrying out welding cycles with one or two current pulses. This characteristic facilitates the welding of parts with some traces of oxide or protective coating. The first pulse pickles the piece and the second pulse consolidates the welding point. The parameters of each one of the impulses (current and time) as well as the interval between impulses (cold) can be regulated separately.

As commented, not all the welding values are obtained by physical experiments, some of them are obtained by simulation after validating the model with some experiments.

Therefore, we have 3 types of pressures (P1, P2 and P3 from less pressure to more pressure), 5 intensities (measured in percentage 40, 50, 60, 70 and 80%) and 3 welding times (T1, T2, T3 from less to more duration of time). It will be made for the union of fine nominal diameters (8+8=16 mm), medium (12+12=24 mm) and thick (16+16=32 mm).

The joining rods are pressed together by the electrodes of the welding machine so that they make good electrical contact. So, you pass electric current through them, they heat up until they start to melt at the point where they are in contact, that's when the molten metal of the two pieces flows and the pieces come together, the current turns off and the molten metal solidifies, forming a solid metallic connection between the two pieces. The welding carried out is spot welding, so that the pieces are welded by small isolated and spaced circular areas, due to their small size, they are called points.

Therefore, we are going to have 45 different unions to be studied and worked on.

Taking into account the aforementioned, each union has a different encoding, following this nomenclature:

$$d - A - T - P$$

Where: d is the thickness of the joint; A is the Intensity; T is the time, and P is the pressure.

Once all the combinations mentioned above have been welded. We proceed to obtain the maximum temperature reached during the welding process in all combinations.

To model this temperature, a computer program and a thermographic camera have been used. The method of obtaining the temperature consists of two steps:

In the first place, the welding processes were recorded with a thermographic camera, which allows us to obtain the temperature values in each case. Once all the videos were obtained, a computer program (FLIR

Tools) was used, with which it was possible to obtain the maximum temperature in each Frame. Table 3 indicates the relationship of the frames with the recording time scale.

Table 3. Frames/Seconds Ratio

Frames	1	5	10	15	20	25	30	35	40	45	50	100	200
Seconds	0.02	0.1	0.2	0.3	0.4	0.5	0.6	0.7	0.8	0.9	1	2	4

However, the maximum temperature that the thermal imager could capture was 670 °C. This made necessary a second step, complementing its full scale through extrapolation in order to identify the heating and cooling curves at the welding points. is the maximum temperature in each frame of the video.

Below is an example of the steps taken to obtain the maximum temperature in a specific case. The values of the Flir tools program are exported to an Excel sheet.

It is checked if the values reach the maximum temperature capable of detecting the thermographic camera (670 °C). If the temperature is lower, you already have the correct data.

However, if the limit of the chamber is reached, the Excel shows the value of 670 °C, so an extrapolation would have to be carried out to obtain the maximum theoretical temperature [5].

To obtain it, the maximum values (670 °C) are eliminated and both the welding heating and cooling curves and the equations of said curves are obtained (figure 2, heating-top and cooling-bottom).

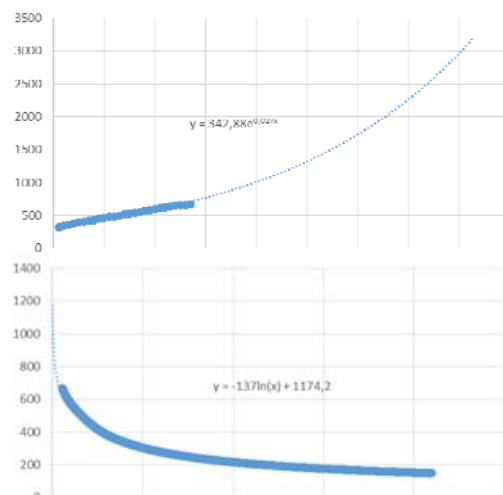


Figure 2. Heating and cooling curve

All the Frames are substituted in these equations and the temperatures for the heating and cooling of the weld are obtained. The cooling and heating values are compared and in the Frame that is closest to the temperatures, an average of both is made and that is the maximum temperature.

Once the extrapolation was carried out in all the combinations and after analyzing the data, it was possible to obtain the maximum temperature of each combination. These temperatures do not have to exceed the maximum values that modify the mechanical characteristics of the corrugated bar steel.

#### 4. Results and Discussion

The first thing is to know up to the maximum temperature that can be reached without changing the properties of the steel. To obtain this temperature, look at the Steel-Carbon Diagram (figure 1), taking into account that the steel used has a carbon percentage of 0.22%. The approximate maximum temperature that can be reached in the welding process for this steel is 1450°C, because from this temperature the steel begins to turn liquid. However, the proper temperature for annealing a hypoeutectoid steel is about 40°C above the critical line. Therefore, it would be advisable not to exceed a temperature of approximately 940°C [5].

The results obtained from the 45 tests with the different pressures, times and intensities for the three joint thicknesses 16, 24 and 32 mm are studied. The results are shown in graphs for each of the thicknesses, in order to make a comparison between the different variables of fusion welding.

Figures 3, 4 and 5 show the graph for the different welding thicknesses. In these, the temperature in degrees Celsius that we reach in the welds is shown on the “Y axis”. On the other hand, the “X axis” shows the intensities in percentage. Each of the alternatives for both time and pressure are shown with their characteristic curve with different lines, as indicated in the legend of the graph. Figure 3 shows the maximum temperature reached depending on the alternative for joints with a thickness of 16 mm.

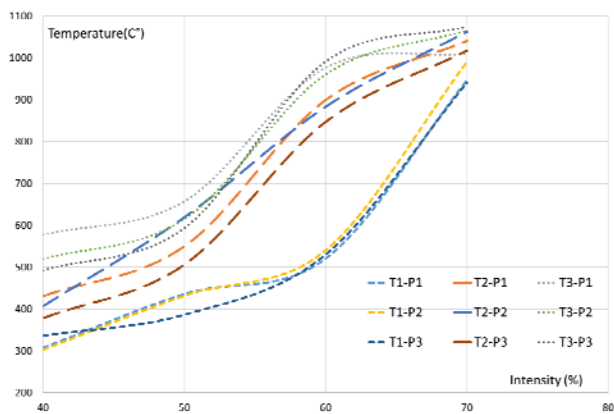


Figure 3. Heating curve depending on the variables for a 16 mm joint (T is time, and P is pressure)

In this graph it should be noted that with intensities of 80%, regardless of time or pressure, the material melts completely making defective welds. The temperature range goes from 300°C to 1080°C.

Pressure effect is not very pronounced, it affects more time. As can be seen for time T1 the increase in temperature is more pronounced from 60 to 70%. On the other hand, for times T2 and T3, the temperature undergoes a large increase between 50 and 60%. On the other hand, as has been mentioned, the pressure does not generate large changes in temperature for the T1 and T3 cases, increasing the range for the T2 cases.

Figure 4 shows the maximum temperature reached depending on the alternative for joints with a thickness of 24 mm.

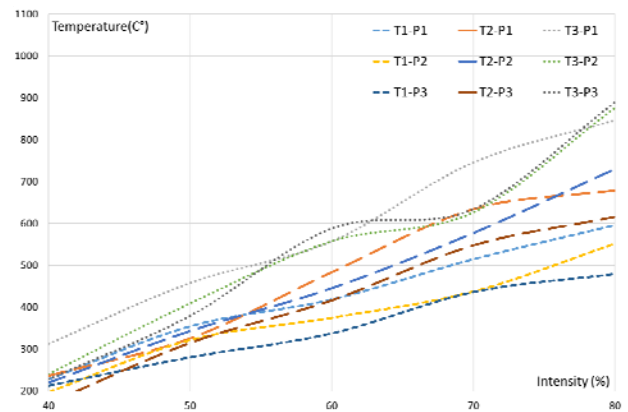


Figure 4. Heating curve depending on the variables for a 24 mm joint

In this graph the temperature range goes from 200°C to 900°C. We can see all the case studies that increase their maximum temperature in a linear and progressive way. The more we increase the pressure, we obtain lower temperatures in the welds. It is observed that the longer the time, the higher the temperatures, with temperatures ranging from 480°C for the T1-P3 case to 890°C for the T3-P3 case with an intensity of 80%. For low intensities the range between temperatures is smaller than for high intensities.

Figure 5 shows the maximum temperature reached depending on the alternative for joints with a thickness of 32 mm.

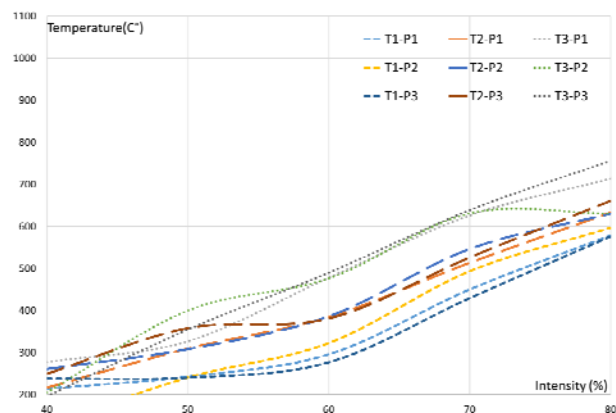


Figure 5. Heating curve depending on the variables for a 32 mm joint (T is time, and P is pressure)

In this graph the temperature range goes from 200°C to 760°C. The temperature increase is kept practically constant up to intensities of 60%, from this value the temperature increase is considerable. But as in the previous graph, the temperature increases in a linear and progressive way. The temperature dispersion is the smallest of the three graphs, reaching a maximum temperature variation of 150°C. It is observed that the longer the time, the higher the temperatures.

## 5. Conclusions

In 100% of the cases studied, the maximum temperature reached is below the melting temperature, that is, 1450°C. However, for each combination a different pressure and intensity would be recommended. In thicknesses of 16 mm, it is recommended to make the welds with an intensity of up to 60 A, a pressure of 6 bars and a low welding time of T<sub>1</sub>, to avoid fusion problems in the weld. For thicknesses of 24 mm, the recommended data is with a welding intensity of 70 A, the pressure in these cases is not very relevant. For thicknesses of 32 mm, high currents are needed, the best being 80 A and short welding times, the working pressure is not very relevant.

The final conclusion is that the fusion welding process is totally valid for rebar welding from the thermal study of welding. And from the point of view of environmental pollution, fusion welding is more recommended because it produces fewer emissions that are harmful to the environment and to humans.

## References

- [1] E. Fraile-García, J. Ferreiro-Cabello, E. Sodupe-Ortega, and A. Sanz-García, "Combined assessment of the environmental, economic and social impacts of structural solutions for residential construction," *Inf. la Construcción*, vol. 67, no. 539, p. e101, 2015.
- [2] J. Ferreiro Cabello, E. Fraile Garcia, E. Martinez de Pison, and E. Jimenez Macias, "Structural alternatives with one way slab in residential buildings," *DYNA*, vol. 90, no. 3, pp. 491–502, 2015.
- [3] E. Fraile-García, J. Ferreiro-Cabello, A. Pernia-Espinoza, and F. J. Martínez-de-Pison, "Technical-economic assessment of redesigned reinforced concrete pre-slabs: Incorporating corrugated cardboard," *Struct. Concr.*, vol. 20, no. 4, 2019.
- [4] E. Fraile-García, J. Ferreiro-Cabello, F. J. Martínez De Pison, and A. V. Pernia-Espinoza, "Effects of design and construction on the carbon footprint of reinforced concrete columns in residential buildings," *Mater. Constr.*, vol. 69, no. 335, 2019.
- [5] E. Fraile-García, J. Ferreiro-Cabello, D. S. Prado, and E. Jiménez, "Assessment and Impact of CO<sub>2</sub> Emissions Attributable to Rebar Used in Building Columns to Withstand Climatic Loads," in *32nd European Modeling & Simulation Symposium, 2020*, pp. 376–386.
- [6] Pérez de la Parte, M., Espinel Hernández, A., Sánchez Orozco, M. C., Sánchez Roca, A., Jiménez Macías, E., Blanco Fernández, J., & Carvajal Fals, H. (2022). Effect of zinc coating on delay nugget formation in dissimilar DP600-AISI304 welded joints obtained by the resistance spot welding process. *International Journal of Advanced Manufacturing Technology*, 120(3-4), 1877–1887. doi:10.1007/s00170-022-08849-2
- [7] Izquierdo, D. R., Álvarez, M. E. G., Roca, A. S., Orozco, M. S., Fernandez, J. B., Fals, H. C., & Macias, E. J. (2020). Stability analysis of the tig-mig hybrid welding process based on digital signal processing. Paper presented at the 32nd European Modeling and Simulation Symposium, EMSS 2020, 410–415. doi:10.46354/i3m.2020.emss.059
- [8] Veitía, B. D. R., Hernández, A. E., Villarinho, L. O., Orozco, M. S., Roca, A. S., Fals, H. C., & Macias, E. J. (2020). Deep learning for quality prediction in dissimilar spot welding DP600-AISI304, using a convolutional neural network and infrared image processing. Paper presented at the 32nd European Modeling and Simulation Symposium, EMSS 2020, 393–399. doi:10.46354/i3m.2020.emss.057
- [9] de la Parte, M. P., Azofra, J. C., Fals, H. D. C., Roca, A. S., Orozco, M. C. S., & Macías, E. J. (2019). A new way to predict the mechanical properties of friction stir spot welding for al-cu joints by energy analysis of the vibration signals. *International Journal of Advanced Manufacturing Technology*, 105(1-4), 1823–1834. doi:10.1007/s00170-019-04396-5
- [10] Colmenero, A. N., Orozco, M. S., Macías, E. J., Fernández, J. B., Muro, J. C. S. -, Fals, H. C., & Roca, A. S. (2019). Optimization of friction stir spot welding process parameters for al-cu dissimilar joints using the energy of the vibration signals. *International Journal of Advanced Manufacturing Technology*, 100(9-12), 2795–2802. doi:10.1007/s00170-018-2779-y
- [11] Jiménez-Macías, E., Sánchez-Roca, A., Carvajal-Fals, H., Blanco-Fernández, J., & Martínez-Cámara, E. (2014). Wavelets application in prediction of friction stir welding parameters of alloy joints from vibroacoustic ANN-based model. *Abstract and Applied Analysis*, 2014 doi:10.1155/2014/728564
- [12] Macías, E. J., Roca, A. S., Fals, H. C., Fernández, J. B., & Muro, J. C. S. -. (2013). Neural networks and acoustic emission for modelling and characterization of the friction stir welding process. [*Emisión Acústica y Redes Neuronales para Modelado y Caracterización del Proceso de Soldadura por Fricción Agitación*] *RIAI - Revista Iberoamericana De Automatica e Informatica Industrial*, 10(4), 434–440. doi:10.1016/j.riai.2013.09.003